RELATIONSHIP BETWEEN MODELLED TURBULENCE PARAMETERS AND CORROSION PRODUCT FILM STABILITY IN DISTURBED SINGLE-PHASE AQUEOUS FLOW

[1]J.POSTLETHWAITE, [1]Y. WANG, [1]G. ADAMOPOULOS AND [2]S. NESIC
[1]*Department of Chemical Engineering*
University of Saskatchewan
Saskatoon, SK
Canada, S7N OWO

[2]*Institutt for energiteknikk*
N 2007 Kjeller
Norway

ABSTRACT. The disruption of corrosion films formed on copper in flowing aerated 3% NaCl solution has been studied in a flow cell with a rectangular cross section, 50 mm wide x 15 mm. The 140 mm long copper deck and the symmetrical acrylic cover had backward and forward facing 2 mm steps to form a constriction resulting in disturbed flow at the leading edge of the sudden constriction and the sudden expansion. The velocity range based on the unconstricted cross section of the flow cell was 0.3-1.5 m s^{-1}*. The development and destruction of the corrosion product films were observed through the transparent cell top. The resulting interactions between the disturbed flow and the films are discussed in terms of the near-wall turbulence parameter profiles, along the length of the flow ceil, calculated by the application of a 2-equation turbulence model with low Reynolds number closure.*

1. Introduction

The effect of single-phase aqueous fluid flow on the stability of corrosion product films is a very important factor in determining the utility of many alloys for applications in process piping systems, resulting in velocity limits and restricted throughputs. Film disruption can be brought about by erosion and/or dissolution [1-3]. The rates of both these film removal mechanisms will be strongly influenced by the structure of the fluid flow with the highest rates of both erosion and mass transfer found under conditions of disturbed flow conditions at bends, weld beads, heat exchanger tube inlets and other sudden changes in the flow geometry. Under such flow conditions the application of the bulk flow parameters, velocity, Reynolds number and wall shear stress(based on the bulk velocity) as the criterion for film disruption is not appropriate. Turbulence models can be used to calculate both the local levels of turbulence and the rates of mass transfer under disturbed flow conditions, providing the local parameters appropriate for the development of film disruption [4-7].

K. R. Trethewey and P. R. Roberge (eds.), Modelling Aqueous Corrosion, 297–316.

This paper describes the application of a k-ϵ, turbulence model to calculate both the local near-wall turbulence profile and the mass-transfer-rate profile along the length of a copper specimen corroding under disturbed flow conditions and relates the profiles to the observed film disruption. Copper tubing often suffers from erosion at elbows and our observations have shown that in some cases the turbulence caused by the step at the downstream tube initiated the film breakdown and corrosion which can be worse in the outlet pipe than the elbow itself. As pointed out recently by A. Cohen [8] in practice the tube ends should be reamed.

2. Modelling

The low-Reynolds-number, k-ϵ turbulence model used in the present study enables the calculation of the species concentration field close to the wag within the viscous sub-layer [7] in addition to performing better for recirculating flows in terms of the flow field prediction [9].

2.1. CONSERVATION EQUATIONS

For axisymmetrical flow in 2D Cartesian coordinates

$$\frac{\partial}{\partial x}(\rho V_x \Phi) + \frac{\partial}{\partial y}(\rho V_y \Phi) = \frac{\partial}{\partial x}(\Gamma_\Phi \frac{\partial \Phi}{\partial x}) + \frac{\partial}{\partial y}(\Gamma_\Phi \frac{\partial \Phi}{\partial y}) + S_\Phi \qquad (1)$$

where $\Phi = V_x, V_y, k, \epsilon, m$

The values of Γ_Φ, general diffusion coefficients and S_Φ, the source terms, are given in Table 1. The effective viscosity is given by:

$$\mu_{eff} = \mu + \mu_t \qquad (2)$$

where the turbulent viscosity, μ_t, is determined from the kinetic energy of turbulence and its rate of dissipation:

$$\mu_t = C_\mu f_\mu \frac{\rho k^2}{\epsilon} \qquad (3)$$

The effective diffusivity is given by:

$$D_{eff} = \frac{\mu}{\rho Sc} + \frac{\mu_t}{\rho \sigma_t} \qquad (4)$$

where σ_t is the turbulent Schmidt number.

TABLE 1
Conservation equations

Conservation of:	Φ	Γ_Φ	S_Φ
Mass	1	0	0
Momentum(x)	V_x	μ_{eff}	$\frac{\partial}{\partial x}\left(\mu_{eff}\frac{\partial V_x}{\partial x}\right)+\frac{\partial}{\partial y}\left(\mu_{eff}\frac{\partial V_y}{\partial x}\right)-\frac{\partial P}{\partial x}$
Momentum(y)	V_y	μ_{eff}	$\frac{\partial}{\partial x}\left(\mu_{eff}\frac{\partial V_x}{\partial y}\right)+\frac{\partial}{\partial y}\left(\mu_{eff}\frac{\partial V_y}{\partial y}\right)-\frac{\partial P}{\partial y}$
Turbulence Kinetic energy	k	$\frac{\mu_{eff}}{\sigma_k}$	$P_k-\rho\varepsilon$
Turbulence dissipation rate	ε	$\frac{\mu_{eff}}{\sigma_\varepsilon}$	$\frac{\varepsilon}{k}(C_{\varepsilon 1}f_1P_k-C_{\varepsilon 2}f_2\rho\varepsilon)$
Species	m	ρD_{eff}	0

$$P_k=\mu_{eff}\left\{2\left[\left(\frac{\partial V_x}{\partial x}\right)^2+\left(\frac{\partial V_y}{\partial y}\right)^2\right]+\left(\frac{\partial V_x}{\partial y}+\frac{\partial V_y}{\partial x}\right)^2\right\}$$

The standard model constants used in the above equations are

$C_\mu=0.09$ $\quad C_{\varepsilon 1}=1.44$ $\quad C_{\varepsilon 2}=1.92$
$\sigma_k=1.0$ $\quad \sigma_\varepsilon=1.3$ $\quad \sigma_t=0.9$

2.2. BOUNDARY CONDITIONS

Since the set of equations is elliptical it is necessary to define boundary conditions for all variables on all boundaries of the computational domain, inlet, walls axis and exit. The low-Reynolds-number damping functions of Lam and Bremhorst [10] were used in the near wall region to modify the turbulence as the wall is approached. At the wall the boundary conditions for k and ϵ, were k = 0, and $\partial\epsilon/\partial y$ = 0.

At the inlet the profile of the mean axial velocity was taken to be fully developed. The turbulence parameters were expressed via the turbulence intensity ($T_{vx} = v'/V_x$), and for the inlet boundary condition T_{vx} data was converted into the k and ϵ values by assuming the length scale, L_e ,equal to half the height of the duct inlet, T_{vx} = 0.05 and

$$k=(3/2)\,T_{v_x}^2 V_x^2 \quad ; \quad \varepsilon=C_\mu^{0.75} k^{1.5}/L_e \qquad (5)$$

In the case of axisymmetric flow, $V_y = 0$ and $\partial\Phi/\partial y = 0$ on the axis. At the outlet, zero gradient boundary conditions were specified for all transport variables.

3. Experimental

The acrylic flow cell (Figure 1) had a rectangular cross section with a flow channel 50.8 mm wide x 15 mm deep, equivalent diameter, d_e = 23.2 mm. The entrance length was 40 d_e and the exit length 20 d_e. The copper deck and the symmetrical acrylic cell cover had backward and forward facing 2 mm steps to form a constriction with de = 18.1 mm. The flow cell was located horizontally in a recirculating flow loop comprising: a rubber centrifugal pump, double pipe heat exchanger, orifice plates, and an open vertical tank used to maintain the solution fully aerated.

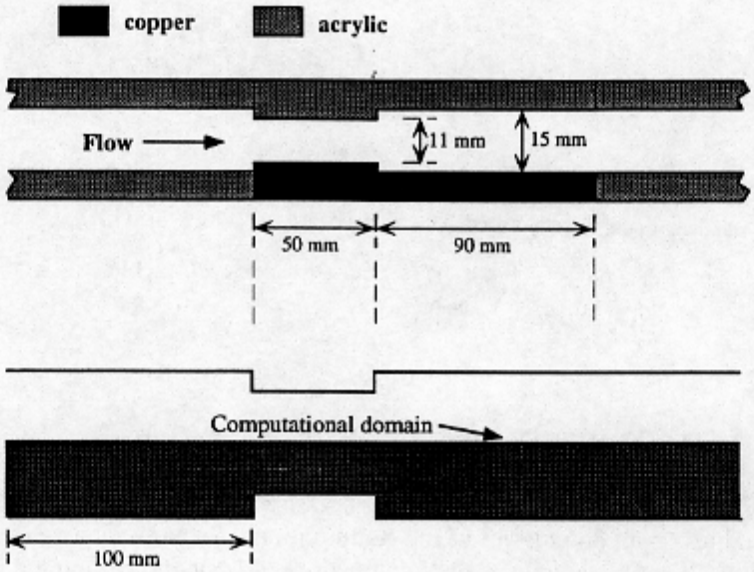

Figure 1 - Flow cell and computational domain.

The copper deck was machined from 99.99% purity electrolytic copper plate. The test solution was aerated 3 wt % NaCl. The bulk velocity, V_b based on the unconstricted cross section, was in the range 0.3 - 1.5 m s^{-1}. The development and destruction of the corrosion product films were observed through the transparent flow cell lid.

4. Results

4.1. FILM REMOVAL AT 44 °C

Films that grew at V_b = 0.5 m s^{-1} (Re = 1.44 x 10^4) were found to be removed (Figure 2) at 1.0 - 1.47 m s^{-1} (Re = 2.88 x 10^4 - 4.23 x 10^4). The Reynolds numbers in the constriction were x 1.36 these latter values. Details of the film removal are given in Table 2.

4.2. FILM REMOVAL AT 25 °C

Films that had been grown at 25 °C and V_b = 0.27 m s^{-1}, for a period of 11 days were stripped rapidly from substantial areas of the surface (Figure 3) when the velocity was raised from 0.27 to 1.49 m s^{-1}. The initial rapid stripping, which occurred minutes after the velocity was raised, has been observed on some other copper samples and obviously occurred by a mechanical mechanism, as opposed to dissolution. The process subsequently progressed more slowly over the next five days until all the metal surfaces, with the exception of a band of film immediately downstream of the expansion, had a metallic pink colour. The reason for the difference between this behaviour and that described in Table 2 is considered to relate to the fact that the films in this experiment were thicker and more prone to mechanical damage. In other experiments at 25 °C the film removal process was slow throughout. The experiments so far completed at 25 °C have shown that film growth is reversed at velocities down to 0.8 m s^{-1} in the present system and it is considered that the critical value at the leading edge of the constriction may be much lower than this.

5. Discussion

The observations made are now discussed in relation to the modelled turbulence parameters. The discussion, except where noted, is concerned with the results in Table 2.

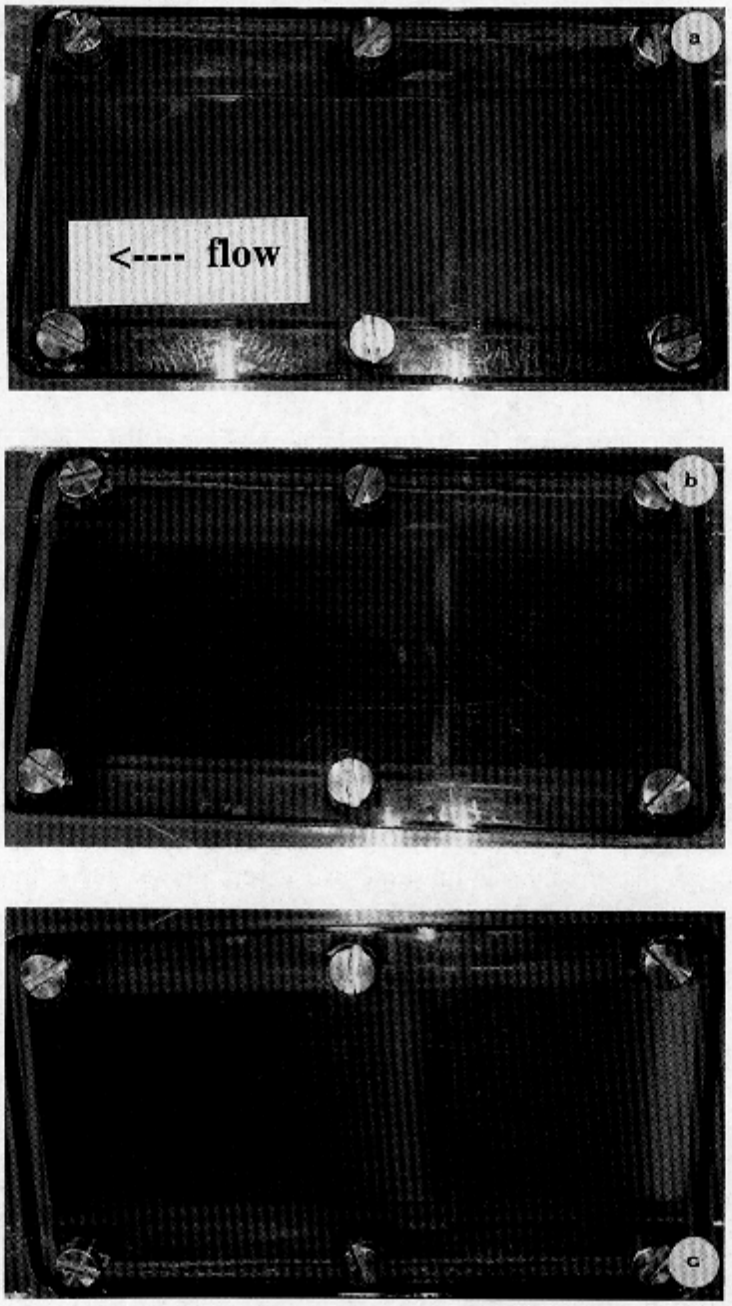

Figure 2 - see next page

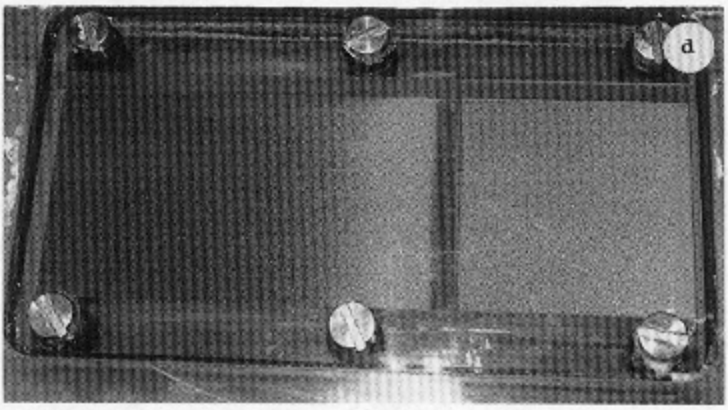

Figure 2 - Removal of corrosion films at 44 °C. a: 0.5 m s^{-1}, day 7; b: 1.0 m s^{-1}, day 17; c: 1.47 m s^{-1}, day 21; d: 1.47 m s^{-1}, day 27. Very slow film removal with no peeling.

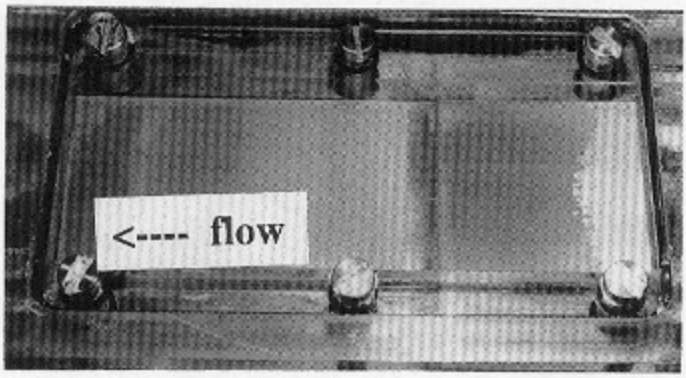

Figure 3 - Removal of corrosion films at 25 °C showing rapid film removal within minutes of raising velocity from 0.27-1.49 m s^{-1}. Film peeling is indicated.

TABLE 2
Growth and removal of corrosion films at 44 °C

Time /days	V /(m s^{-1})	Corrosion films
14	0.5	Dark brown corrosion film grew over most of the exposed surfaces leaving a small lighter coloured 2 mm wide band of film at the leading edge of the sudden constriction which was subjected to a small amount of pitting.
14-17	1.0	Very slow thinning of films observed with a spread of the 2 mm band at the leading edge downstream. The colour of this band was now metallic pink and the film removal obvious. There was also the formation of a light coloured band suggesting film thinning 12 mm wide starting ca. 6 mm downstream of the sudden expansion with a few pits.
17-34	1.47	The thinning continued with complete clearance of the film in the constriction by day 26. By day 26 the film downstream of the sudden expansion had been removed from a 24 mm band starting at 6 mm downstream of the sudden expansion. The film remained intact in a 5 nun band immediately downstream of the sudden expansion until the end of the experiment on day 34. A small amount of green corrosion products formed in the comer of the sudden expansion. At the end of the experiment the duct wide band of complete film removal in the expansion zone starting from 5 mm downstream of the sudden expansion was 29 mm long and followed by a zone some 25 mm long where the film was considerably thinned in an uneven manner.

5.1. STRUCTURE OF FLOW

Film disruption started at the leading edge of the sudden constriction and just downstream of the sudden expansion, two places where the greatest near-wall turbulence would be expected to occur.

Figure 4 is a schematic of the flow structure. The three parameters that could be possibly be related to film disruption near-wall turbulence, wall shear stress and the mass transfer coefficient are shown in detail for the sudden constriction (Figure 5) and sudden expansion (Figure 6) for V_b = 1.47 m s^{-1}. The distances in the figures relate to the x direction in the computation zone which was longer than the copper deck to enable the assumption of fully developed flow at the inlet and outlet of the computation domain. The distance x = 100 mm corresponds to the start of the copper deck, and the position along the copper deck can be seen in the figures.

Examination of the wall shear stress profile reveals the structure of the flow. Points where values of τ_w change sign correspond to flow reversal. Flow reversal relates to flow separation with recirculation and reattachment.

At the sudden constriction (Figure 5) recirculating flow is predicted in the comer immediately prior to the constriction and at the entrance to the constriction with the latter flow separating at x = 100.5 mm and reattaching at 105 mm. At the sudden expansion (Figure 6) the separated flow which separates at the edge of the expansion reattaches at x =162.5 mm. There is also a small recirculating flow in the comer.

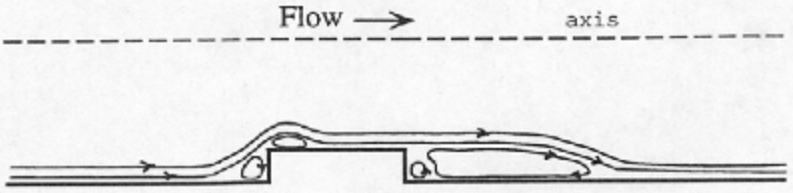

Figure 4 - Schematic diagram of flow structure.

The location where the film remained intact throughout the 34 day experiment was 150-155 mm, and from 194 mm to the end of the system The film was completely removed from the constriction, 100-150 mm, and from 155-174 mm downstream of the constriction. The film was thinned unevenly from 174-199 mm to a zone of thinned film starting at x = 174 - 194 mm.

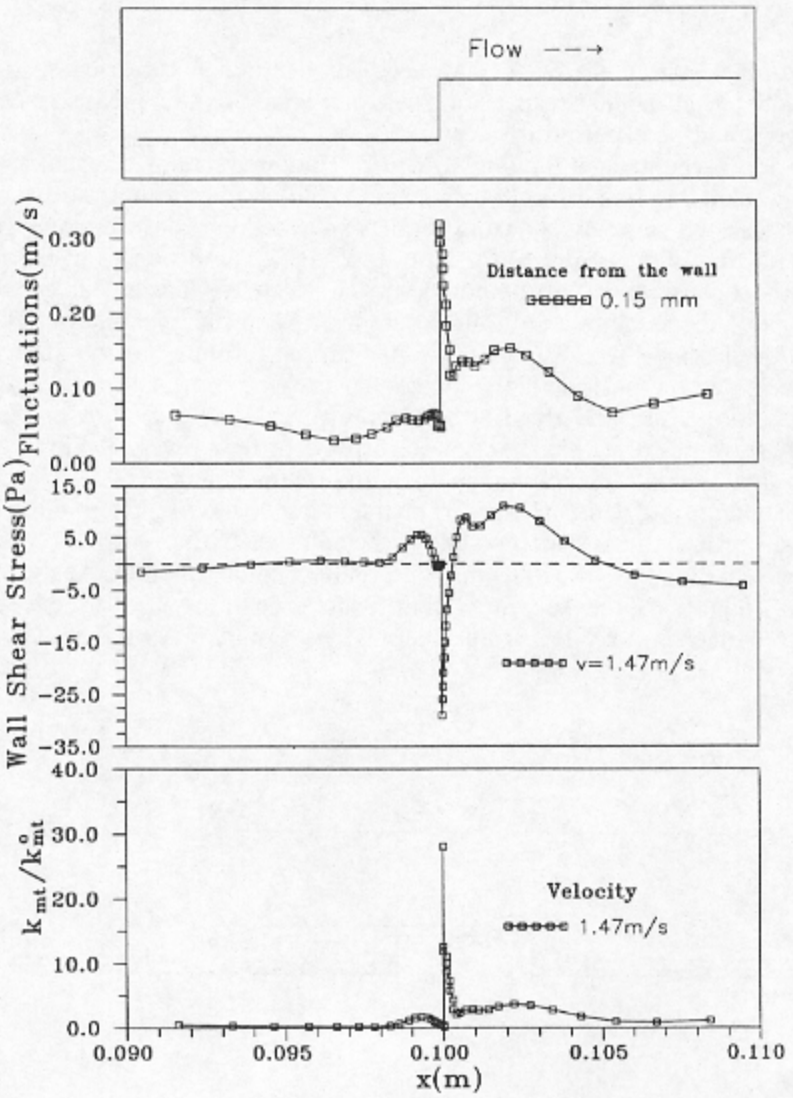

Figure 5 - Predicted velocity fluctuations, wall-shear stress and mass transfer coefficients at the sudden constriction (backward facing step).

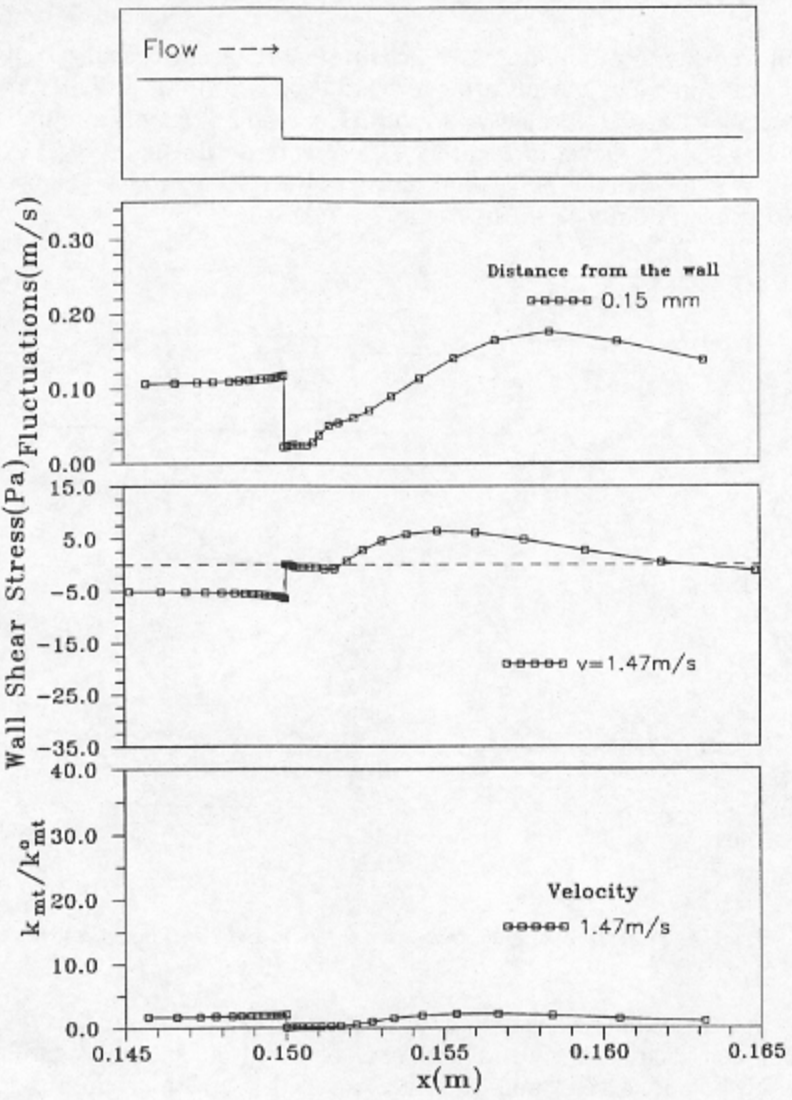

Figure 6 - Predicted velocity fluctuations, wall shear stress and mass transfer coefficients at the sudden expansion (forward facing step).

5.2. NEAR-WALL TURBULENCE

Near-wall velocity fluctuations, v', which are more easily visualized than the corresponding kinetic energy of turbulence are used here to quantify the near-wag turbulence. The calculated values of V_b at 0.15 mm and at I mm from the wall for V_h = 1.47 m s^{-1}, are shown in Figure 7. These velocity fluctuations (RMS) were calculated from the kinetic energy of turbulence given by the model. The k-ϵ models assume isotropic turbulence stresses and v' =√(2k/3).

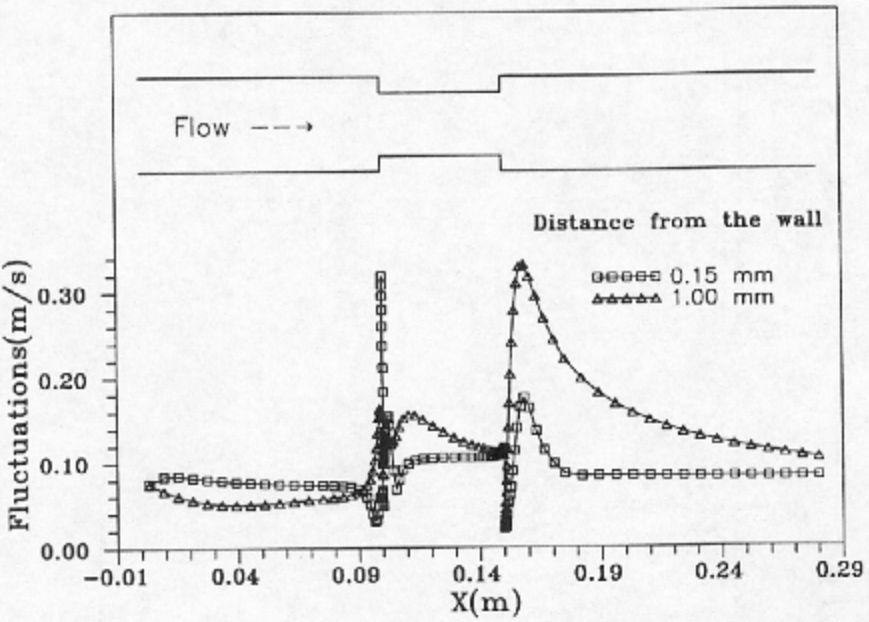

Figure 7 - Predicted velocity fluctuations at 0.15 mm and 1 mm from the wall at 1.47 m s^{-1} and 44 °C.

The near-wall turbulence is greater at 0. 15 mm than at 1 mm from the wall at the sudden constriction in contrast to the behaviour at the sudden expansion. The enhanced turbulence level 1 mm from the wall at the sudden expansion relates to the transport of the turbulence downstream from the point of flow separation. The latter enhanced turbulence is damped as the wail is approached. Close to the wall, where the turbulence can have the greatest effect on the stability of films, the level of turbulence at the sudden constriction, is much higher than that at the sudden expansion. In previous studies [4, 11] the turbulence at 12 mm was used to study the effect of turbulence in a similar geometry. The present results indicate the care that should be taken in the choice of wall distance for determining the near-wall

turbulence level if the latter is to be used as a criterion for film stability. Conclusions based on the 0.15 mm calculations are in agreement with the observations whereas the results for 1 mm show the opposite.

The velocity fluctuations for the three velocities used are shown in Figure 8. If velocity fluctuations can be used as a criterion for film removal the following assumptions can be drawn. For the leading edge complete film growth was prevented where the predicted fluctuations at V_b = 0.5 m s^{-1} are 0.1 m s^{-1}. Fluctuations of 0.17 m s^{-1} at V_b = 1.0 m s^{-1} initiated the slow removal of the film at the leading edge of the constriction. The fluctuations at V_b = 1.47 m s^{-1} permitted the complete removal of the film in the constriction. For the sudden expansion, film thinning was observed in the presence of fluctuations of 0.08 m s^{-1} at V_b = 1.0 m s^{-1}. Downstream of the sudden expansion the film removal rate became very low when the removal reached x = 184 mm where the fluctuations were below 0.09 m s^{-1}.

If a critical value of modelled velocity fluctuations were to be chosen for copper in the present system it would be around 0.1 m s^{-1}.

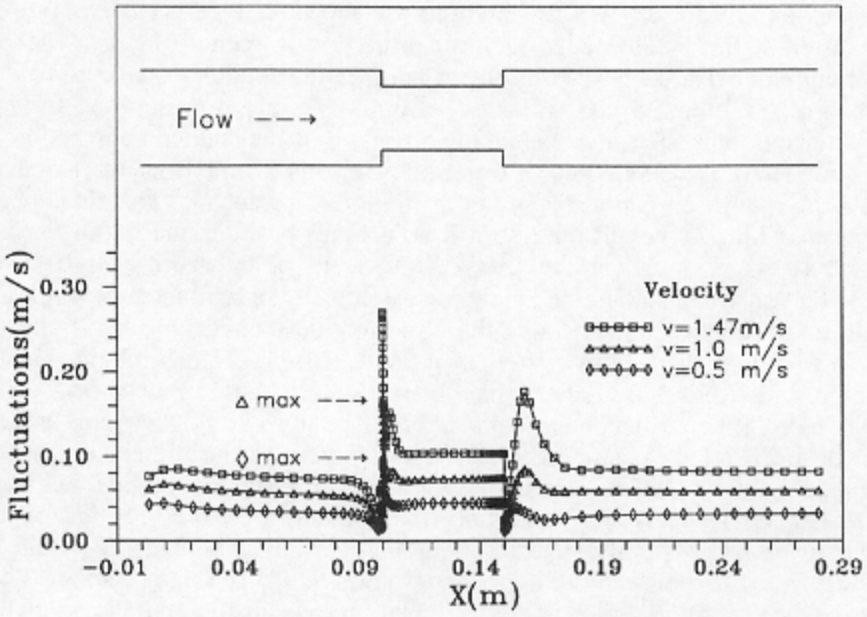

Figure 8 - Predicted velocity fluctuations 0.15 mm from the wall at bulk velocities of 0.5, 1.0 and 1.47 m s^{-1}.

5.3. WALL SHEAR STRESS

The wall shear stress values at V_b = 0.5 - 1.47 m s^{-1} at the leading edge of the sudden constriction, Figure 9, exceed the value of 9.6 Pa reported by Efird [12] for

the accelerated corrosion of the 99.9% Cu alloy CDA 122, due to the degradation and physical removal of protective films. The values in the small recirculation zone just downstream of the leading edge of the constriction are also >9.6 Pa at 1.47 m s^{-1}. The maximum downstream of the expansion at x = 155 mm corresponds to the starting position for complete film removal at 1.47 m s^{-1}. Having said this it must be noted that several [13-15] have questioned whether the small values of τ_w said to be responsible for film disruption are indeed capable of physically removing tightly adherent protective films and the values calculated for the present system, even at the points of disturbed flow, are small.

5.4. MASS TRANSFER

It was not obvious in this particular experiment (Table 2) whether mechanical stripping of the film or dissolution was responsible for the film removal when the velocity was raised. The mass transfer coefficients calculated on the basis of the transfer of a species with a Schmidt number of 500 (relevant to the mass transfer of species such as Cu^{2+} in the present solution) are shown in Figure 10. The rate of mass transfer at the leading edge of the constriction is seen to be an order of magnitude greater than at the reattachment point in the sudden expansion. And if dissolution of the film and mass transfer played a role in the present experiment then it is obvious why the film was initially disrupted at the sudden constriction.

Loss and Heitz [16], Syrett [13], Lotz and Heitz [17] and Bianchi [14] have discussed the role of mass transfer in the disruption of protective films on copper. Sydberger and Lotz suggested that there is no analogy between mass transfer and wall shear stress at and near the flow reattachment point where $\tau_w = 0$. They suggested that upstream and immediately downstream of the reattachment point the shear stresses are considerable lower than for fully developed flow. It should be noted however that the highest values of c_μ and near-wall values of the kinetic energy of turbulence in the sudden expansion are in fact found in the recirculation zone upstream of the reattachment point where the values are higher than in fully developed flow (Figure 5). There is some uncertainty about the coincidence of the reattachment point and the position of maximum mass transfer and the reattachment point [19, 20, 7]. There is also some uncertainty about the exact position of the reattachment point itself [21]. And in addition the reattachment point is said to exhibit strong oscillations about its mean position [19]. The film removal that occurred in the expansion started in the recirculation zone upstream of the predicted attachment point corresponding to the region of highest turbulence, wall shear stress and mass transfer in the expansion. The modelled reattachment point at 1.47 m s^{-1} is 12 mm (6 step heights) downstream of the expansion (Figure 5). Lotz and Postlethwaite [11] noted that the maximum rate of mass transfer occurred upstream of the maximum near-wall turbulence that was also the case in the present simulations. The conclusion drawn here is that when mass transfer is involved in the film removal process at a sudden expansion the maximum effect will be observed in

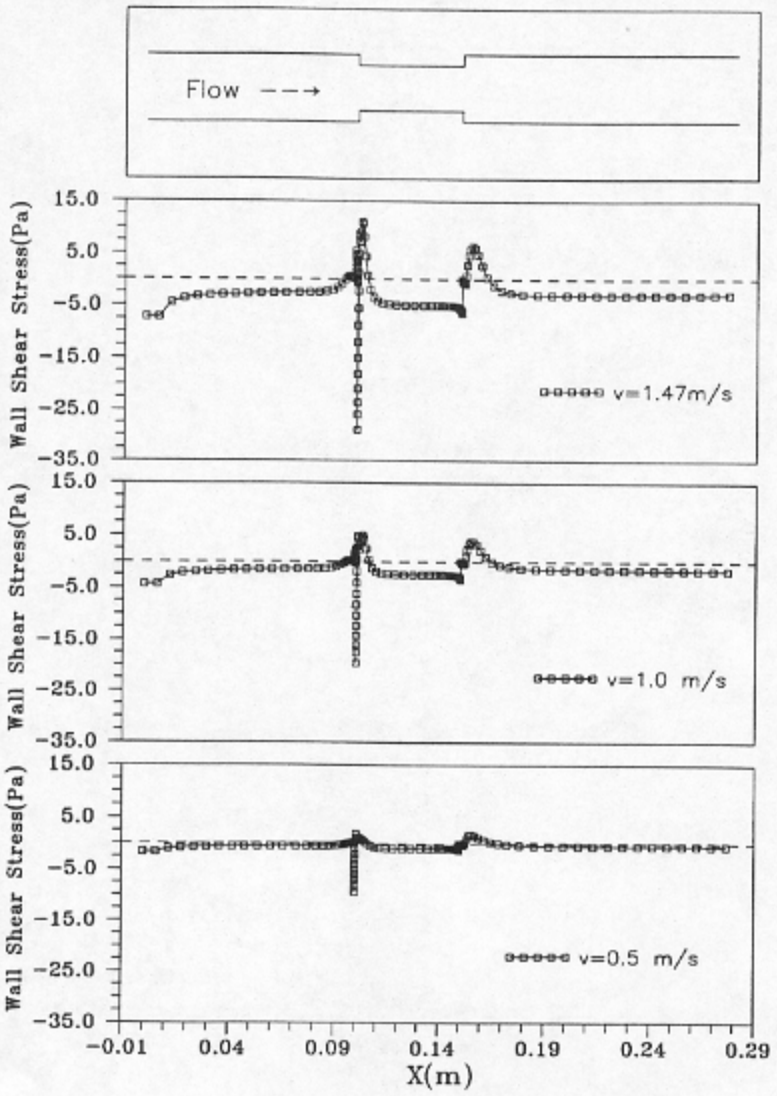

Figure 9 - Predicted wall shear stresses at bulk velocities of 0.5, 1.0 and 1.47 m s^{-1}.

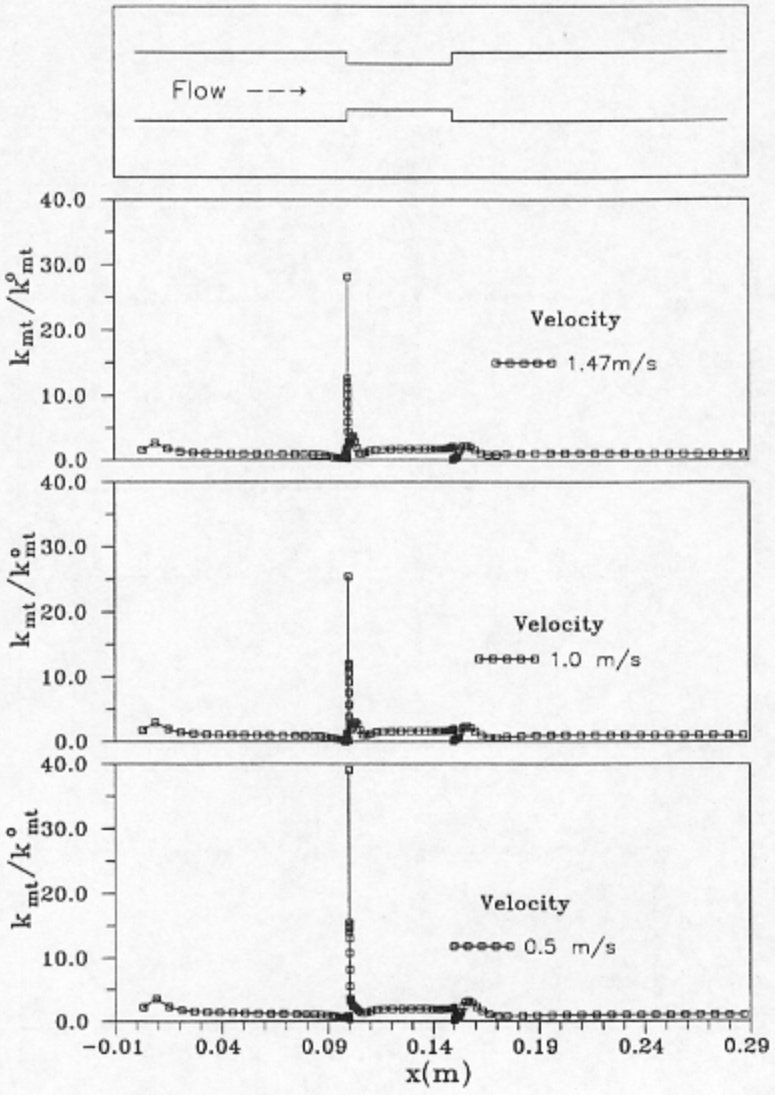

Figure 10 - Predicted mass transfer coefficients at bulk velocities of 0.5, 1.0 and 1.47 m s^{-1}.

the recirculating zone upstream of the reattachment point.

5.5. EFFECT OF TEMPERATURE

The modelled turbulence parameters at 25 °C were not too different to those at 44 °C and only the near-wall fluctuations for 25 °C are presented here (Figure 11) for comparison with the results at 44 °C.

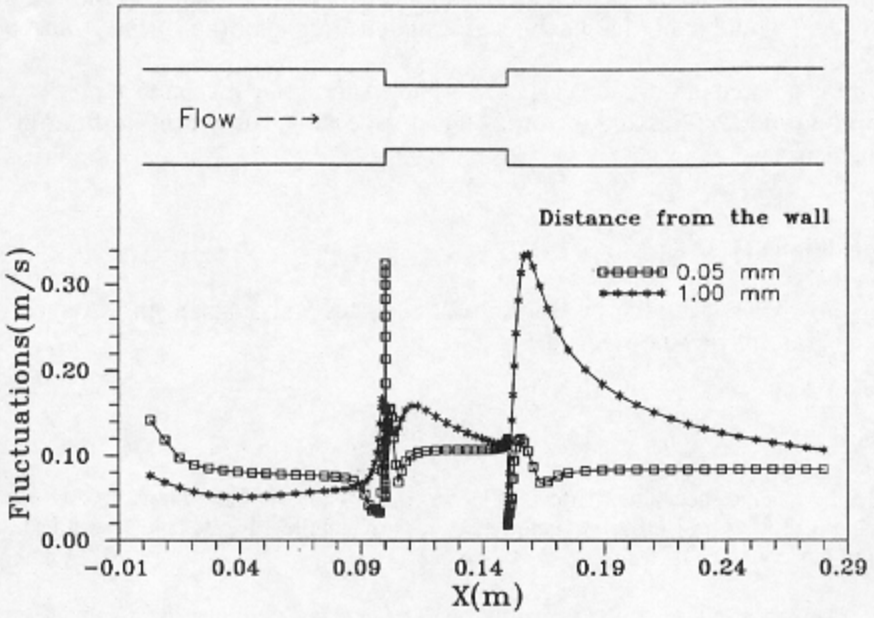

Figure 11 - Predicted velocity fluctuations at 0. 15 mm and 1 mm from the wall at 1.49 m s^{-1} and 25 °C.

5.6. CHOICE OF CRITERIA FOR FILM BREAKDOWN

Although there is obviously a strong relationship between the modelled turbulence parameters and film disruption much work remains to be done before a suitable disruption criterion is selected from the several parameters that can be modelled. Because of the different mechanical and physicochemical properties of the films formed on corroding metals the parameter once selected will have widely varying critical values. Once determined the modelling procedure will determine whether or not the value wig be exceeded at any specified flow rate and in any particular geometry.

The major problem that confronts progress in the identification of a suitable criterion for film disruption by mechanical processes is that the mechanism of film removal and the forces involved are not understood. It should be remembered that directly at the wall there are no velocity fluctuations even if bursting phenomena,2 involving fast eddy ejection, are taken into account. Bursting phenomena can involve the removal of a considerable portion but not all of the viscous sub-layer [22] down to the wail. There are however both shear stress [23] and pressure fluctuations [24] directly at the wall and as discussed by Launder [24] future modelling work in this field should involve the direct numerical simulation of the turbulence in the viscous sub-layer that would lead to a much greater understanding of the surface transport processes.

Finally as pointed out by Heitz [1] little is known about the mechanical properties of corrosion product films and of course this is especially true for *in situ* films on a corroding surface.

Acknowledgements

The support of this research by the Natural Sciences and Engineering Council of Canada is gratefully acknowledged.

References

1. E. Heitz, "Chemo-mechanical Effects of How on Corrosion", in Flow-Induced Corrosion: Fundamental Studies and Industry Experience, K. J. Kennelley, R. H. Hausler and D. C. Silverman, eds., NACE, Houston, 1991, 1-1 to 1-29.

2. J. L. Dawson and C.C. Shih, "Corrosion under Flowing Conditions-An Overview and Model," ibid, 2-1 -2-12.

3. E. F. C. Somerscales and H. Sanatgar, "Hydrodynamic Removal of Corrosion Products From a Surface", *British Corrosion Joumal*, Vol. 27 No. 1, 1992, 36-44.

4. S. Nesic and J. Postlethwaite, "Relationship Between the Structure of Disturbed Flow and Erosion-Corrosion", *Corrosion,* Vol. 46, No 11, 1990, 874-880.

5. H. Zeisel and F. Durst, "Computations of Erosion-Corrosion Processes in Separated Two-Phase Flows," in "Flow-Induced Corrosion: Fundamental Studies and Industry Experience", K. J. Kennelley, R. H. Hausler and D. C. Silverman, eds., NACE, Houston, 1991, 9-1 to 9-21.

6. S. Nesic and J. Postlethwaite, "A Predictive Model for Erosion-Corrosion," *Corrosion,* Vol. 47, No. 8, 1991, 582-591.

7. S. Nesic, J. Postlethwaite and D. J. Bergstrom, "Calculation of Wall Mass Transfer Rates in Separated Aqueous Flow Using a Low Reynolds Number k-ϵ Model", *Int. J. Heat Mass Transfer,* Vol. 35, No. 8, 1992, 1977-1985.

8. A. Cohen, "Corrosion by Potable Water in Building Systems", *Materials Performance*, Vol. 32, No. 8, 1993, 56-61.

9. S. Nesic, G. Adamopoulos, J. Postlethwaite and D. J. Bergstrom, "Modelling of Turbulent Flow and Mass Transfer with Wall function and Low Reynolds Numbers Closures", *Can. J. Chem. Eng.*, Vol. 71, Feb., 1993, 28-34.

10. C. K. G. Lam and K. Bremhorst, "A Modified Form of the k-ϵ Model for Predicting Wall Turbulence", *ASME J. Fluids Eng.*, Vol. 103, 1981, 456-460.

11. U. Lotz and J. Postlethwaite, "Erosion-Corrosion in Disturbed Two Phase Liquid/Particle Flow", *Corrosion Science,* Vol. 30, No. 1, 1990, 95-106.

12. K. D. Efird, "Effect of Fluid Dynamics on the Corrosion of Copper Base Alloys in Sea Water", *Corrosion,* Vol. 33, No. 1, 1977, 3-8.

13. B. C. Syrett, "Erosion-Corrosion of Copper Nickel Alloys in Sea Water and Other Aqueous Environments - A Literature Review", *Corrosion,* Vol. 32, No 6, 1976, 242-252.

14. G. Bianchi, G. Fiori, P. Longhi and F. Mazza, "Horse Shoe Corrosion of Copper Alloys in Flowing Sea Water: Mechanism, and Possibility of Cathodic Protection of Condenser Tubes in Power Stations", *Corrosion,* Vol. 34, No 11, 1978, 396-406.

15. D. D. Macdonald, B. C. Syrett and S. S. Wing, "The Corrosion of Copper Nickel Alloys 706 and 715 in Flowing Sea Water. I - Effect of Oxygen", *Corrosion,* Vol. 34, No 9, 1978, 289-301.

16. C. Loss and E. Heitz, "Zum Mechanismus der Erosionkorrosion in Schnell Strömenden Flüssigkeiten", *Werkestoffe und Korrosion,* Vol. 24, No. 1, 1973, 38-48.

17. U. Lotz and E. Heitz, "Flow Dependent Corrosion. Current Understanding of the Mechanisms Involved", *Werkestoffe und Korrosion,* Vol. 34, 1983, 454-461.

18. T. Sydberger and U. Lotz, "Relation Between Mass Transfer and Corrosion in a Turbulent Pipe Flow", *J. Electrochem. Soc.*, Vol. 129, No. 2, 1982, 276-283.

19. A. K. Runchal, "Mass Transfer Investigafion in Turbulent Flow Downstream of Sudden Enlargement of a Circular Pipe for Very High Schmidt Numbers", *Int. J. Heat Mass Transfer,* Vol. 14, 1971, 781-792.

20. R. S. Amano, "A Study of Turbulent Mass Transport Downstream of an Abrupt Pipe Expansion", *Numerical Heat Transfer*, Vol. 8, 1985, 361-37 1.

21. M. Sdeglmeir, C. Tropea, N. Weiser, W. Nitsche, "Experimental Investigafion of the Flow Through Axisymmetric Expansions", ASME, *J. Fluids Eng.*, Vol. 111, 1989, 464-471.

22. R. Dworak and H. Wendt, "Stochastic Fluctuations of Mass Transport Through Turbulent Boundary Layers", *Ber. Bunsenges. physik.*, Vol. 81, No 9, 1977, 864-869.

23. D. A. Shah and R. A. Antonia, "Scaling of Wall Shear Stress Fluctuations in a Turbulent Duct Flow", *AIAA J.* ,Vol. 25, No. 1, 1986, 22-29.

24. B. E. Launder, "Second - Moment Closure: Present and Future", *Int. J. Heat and Fluid Flow*, Vol. 10, No. 4, 1989, 282-300.